Characteristic trends in the x-ray rates from the 2*s*3*p* configuration of He-like ions

L. Natarajan and Anuradha Natarajan
Department of Physics, University of Mumbai, Mumbai 400 098, India
and Department of Physics, SIWS College, Mumbai, India

(Received 11 November 2008; revised manuscript received 13 April 2009; published 26 June 2009)

Relativistic configuration interaction results are presented for the $K\beta$ x rays from $2s3p$-$1s2s$ transitions in He-like ions. The x-ray energies and rates are calculated for 23 ions in the range $Z=14$ to 54 using multiconfiguration Dirac-Fock wave functions in the active space approximation. The calculations include finite nuclear size effect, Breit interaction, and quantum electrodynamic corrections. The influence of configuration mixing on the converged x-ray rates is analyzed. Our calculations show that strong configuration mixing reduces substantially the single configuration electric dipole allowed as well the $^3\mathrm{P}_1$-$^1\mathrm{S}_0$ spin-forbidden transition rates and its contribution decreases with increasing Z. While configuration mixing consistently reduces the monoconfiguration rate of $^1\mathrm{P}_1$-$^3\mathrm{S}_1$ transition in ions with $Z<22$ by as much as 94%, it enhances the spin-forbidden rate of ions with $Z\geq 23$. The contributions from higher order relativistic corrections are seen to be negligible for $^1\mathrm{P}_1$-$^1\mathrm{S}_0$ and $^1\mathrm{P}_1$-$^3\mathrm{S}_1$ transitions whereas the effect of Breit interaction is appreciable for the other transitions to $^3\mathrm{S}_1$ state, especially for the high-Z ions. The results are compared with other available values.

DOI: 10.1103/PhysRevA.79.062513 PACS number(s): 32.30.−r, 31.15.−p

I. INTRODUCTION

The $K\alpha$ x rays from He-like ions in the mid-Z regions have been observed both in laser produced and tokomak plasmas. The x rays emitted from highly ionized few-electron atoms are proved to be important in determining the various plasma parameters [1–4]. Accurate x-ray energies and rates from few-electron ions have been measured in laser produced plasmas [5], tokomak plasmas [6–10], and beam-foil spectroscopy [11–13]. Relativistic and nonrelativistic calculations on the isoelectronic sequence of He-like to B-like ions with a single K electron and variously ionized L shell configurations have been studied in the past [11,13–17]. However, the $K\beta$, $K\gamma$, etc. x rays coming from $n>2$ to $n=1$ few-electron highly ionized systems have not been explored in detail. It is believed that the transitions corresponding to these spectra are optically thin even in a dense laser plasma and hence could be even more useful for diagnostic applications than the x rays from $n=2$ to $n=1$ transitions [18]. The experimental observations on the $K\beta$ spectrum of He-, Li-, and Be-like iron from tokomak fusion test reactor (TFTR) plasmas have been reported by Smith *et al.* [9]. Similar investigations on argon recorded with high resolution spectrometer on the Princeton Large Taurus tokomak plasmas have been analyzed by Beiersdorfer *et al.* [8]. It was shown that the $K\alpha$ spectrum of He-like Ni and the $K\beta$ spectrum of He-like iron overlap as these elements are simultaneously present in tokomaks like TFTR. The theoretical investigations on the $K\beta$ spectrum of He-like Fe and Ar and the satellite transitions from Li- and Be-like Fe and Ar obtained with HULLAC package have also been carried out by Smith *et al.* [9] and Beiersdorfer *et al.* [8]. The dielectronic satellite spectra of H-like Si, Ar, Ti, Cr, Fe, and Ni have been studied by earlier researchers [19–21] using Hartree-Fock Slater model. Recently, extensive tabulations on the x-ray energies and rates for various transitions from $n=2$ and 3 to $n=1$ and the autoionization rates for doubly excited 2 ln l′ and $1s2$ ln l′ states in ions with atomic numbers $Z=6$ to 36 have been reported by Goryayev and Vainshtein [22]. The calculations were carried out by them using MZ code based on the Z expansion method with the inclusion of relativistic corrections within the framework of the Breit operator. However, detailed analysis of the characteristics of the transition rates from few-electron ions has not been carried out.

In our previous work [23], we have shown that configuration interaction can vary the single configuration rates of $K\beta$ x rays from $2s^2 3p$ and $1s2s^2 3p$ configurations of Li-like and Be-like ions, respectively, by as much as 30%. In continuation of our earlier study, in this paper the effects of configuration mixing on the energies and rates of $K\beta$ x rays from $2s3p$-$1s2s$ transitions in He-like ions are analyzed using multiconfiguration Dirac-Fock (MCDF) wave functions with the inclusion of Breit interaction, self-energy, and vacuum polarization. The finite nuclear size effect has been included in the calculations by considering a two-parameter Fermi charge distribution. The MCDF method is shown to be efficient in treating the correlation effects due to strong interaction of the nearly degenerate excited states with the reference state. For the sake of convenience, nonrelativistic notation is used in many places in the present paper. The correlation effects have been computed by excitation of atomic orbitals in the active space approximation. The calculations have been carried out using GRASPVU code [24,25] for He-like isoelectronic sequence in the range $Z=14$ to 54.

II. NUMERICAL PROCEDURE

In a multiconfiguration relativistic calculation, the configuration state functions (CSFs) are antisymmetrized sum of product of Dirac spinors and the atomic state function is expanded in terms of CSFs,

$$\Psi(\gamma PJM) = \sum c_{it}\varphi_i(\gamma_i PJM). \quad (1)$$

The Dirac spinors and the expansion coefficients are described in detail in literature [26,27]. The theoretical back-

TABLE I. Electric dipole rates of $K\beta$ x rays in s^{-1} in length gauge from states of $2s3p$ configuration in He-like ions with correlation from 15 CSFs. The first row of each element represents the single configuration DF rates, second row lists the rates with only correlation, while the third row gives the rates with QED effects, Breit interaction and correlation. The numbers in parentheses signify powers of ten.

Z	$^1P_1$-$^1S_0$	$^3P_1$-$^3S_1$	$^3P_0$-$^3S_1$	$^3P_2$-$^3S_1$	$^1P_1$-$^3S_1$	$^3P_1$-$^1S_0$
14	5.569(12)	5.673(12)	5.731(12)	5.733(12)	5.801(12)	5.678(12)
	5.592(12)	5.857(12)	5.917(12)	5.917(12)	5.962(10)	5.684(10)
	5.582(12)	5.851(12)	5.913(12)	5.914(12)	6.185(10)	5.889(10)
18	1.526(13)	1.548(13)	1.607(13)	1.606(13)	5.888(11)	5.787(11)
	1.572(13)	1.594(13)	1.655(13)	1.651(13)	6.053(11)	5.937(11)
	1.561(13)	1.582(13)	1.644(13)	1.643(13)	6.217(11)	5.981(11)
21	2.766(13)	2.799(13)	3.014(13)	3.012(13)	2.133(12)	2.100(12)
	2.772(13)	2.856(13)	3.074(13)	3.073(13)	2.171(12)	2.102(12)
	2.760(13)	2.846(13)	3.071(13)	3.069(13)	2.238(12)	2.164(12)
23	3.892(13)	3.934(13)	4.359(13)	4.364(13)	4.270(12)	4.210(12)
	3.982(12)	4.092(13)	4.548(13)	4.546(13)	4.557(12)	4.439(12)
	3.962(13)	4.074(13)	4.542(13)	4.541(13)	4.681(12)	4.55(312)
28	8.013(13)	8.079(13)	9.692(13)	9.675(13)	1.603(13)	1.58(213)
	8.025(13)	8.195(13)	9.827(13)	9.815(13)	1.624(13)	1.584(13)
	7.965(13)	8.144(13)	9.814(13)	9.799(13)	1.660(13)	1.616(13)
36	2.014(14)	2.024(14)	2.674(14)	2.665(14)	6.450(13)	6.372(13)
	2.016(14)	2.045(14)	2.701(14)	2.694(14)	6.511(13)	6.376(13)
	1.998(14)	2.030(14)	2.696(14)	2.687(14)	6.608(13)	6.458(13)
44	4.283(14)	4.287(14)	5.994(14)	5.960(14)	1.683(14)	1.662(14)
	4.294(14)	4.322(14)	6.037(14)	6.097(14)	1.696(14)	1.662(14)
	4.245(14)	4.289(14)	6.023(14)	5.990(14)	1.712(14)	1.676(14)
52	8.126(14)	8.099(14)	1.170(15)	1.159(15)	3.531(14)	3.476(14)
	8.127(14)	8.149(14)	1.176(15)	1.167(15)	3.549(14)	3.476(14)
	8.051(14)	8.089(14)	1.173(15)	1.163(15)	3.575(14)	3.492(14)

ground necessary for the evaluation of x-ray energies and rates using MCDF wave functions including higher order correction terms is described by many workers in the past [26–28].

The construction of near exact atomic state functions using systematic expansion of the orbitals in the active space and the effect of the various orbitals on the transition rates have been discussed in detail in our earlier studies [23,29,30]. In this work, the zero order Dirac-Fock (DF) wave functions were generated from the $2s3p$ and $1s2s$ reference configurations in extended optimal level scheme where the radial orbitals and the mixing coefficients are determined by optimizing the energy functional which is the weighted sum of the energy values corresponding to a set of eigenstates. The succeeding terms were obtained by considering an active space in which the jj-coupled CSFs of a given parity P and J symmetry are generated by excitation of electrons from the reference configuration to the orbitals in the active set.

To analyze the influence of higher order corrections and correlation on the single configuration energies and dipole rates of x rays from $2s3p$ configuration of He-like ions, we performed a series of systematic calculations. We first evaluated the single configuration DF energies and rates of the $K\beta$ lines without taking into account correlation effects and higher order corrections. We then generated 15 CSFs by considering single and double (SD) excitations of electrons from the reference configurations to the $\{1s_{1/2}, 2s_{1/2}, 3p_{1/2}, 3p_{3/2}\}$ orbital set and evaluated the transition energies and rates. In the next step, we included correlation as well as Breit interaction and quantum electrodynamic (QED) corrections on these unfilled spin-orbitals in the reference configurations and evaluated the transition energies and rates. As the single configuration basis set is found to be optimal with SD excitation of orbitals with 15 CSFs, we took advantage of this two-step procedure. Then by gradually expanding the size of the active space, these two sets of calculations, one with only correlation effects (MCDF) and the other with Briet interaction and QED corrections coupled with correlation (RCI) were repeated for each step-by-step multiconfiguration expansion taking care of the convergence criteria which in this work was taken to be 10^{-8}.

The active set considered in this work consisted of orbitals with the principal quantum number n ranging from 1 to 6 that produced 505 CSFs. The $n=1$ to 5 Layzer complex consisted of $l=0$ to 4 spin-orbitals while for $n=6$ Layzer we considered only spin-orbitals with $l=0$ and 1. Further expansion of the active space did not contribute much to the mix-

TABLE II. Energies in a.u. of the various states from $2s3p$ and $1s2s$ configurations in He-like Fe. Column 1 lists the orbitals included in the set. First row of each expanding set lists the energy values with only correlation while the second row includes correlation as well as Breit interaction and QED corrections.

	Energy					
	Initial states				Final states	
Active set	$^3P_0$	$^3P_1$	$^3P_2$	$^1P_1$	$^1S_0$	$^3S_1$
DF	121.091	121.059	120.872	120.763	420.466	421.635
$1s2s3p$	121.090	121.058	120.871	120.762	420.436	421.635
	121.067	121.038	120.850	120.742	420.224	421.471
$\{n2,3p\}$	121.083	121.052	120.864	120.758	420.444	421.636
	121.060	121.031	120.843	120.738	420.233	421.473
$\{n3,3s,3p\}$	121.033	121.104	120.891	120.798	420.475	421.644
	121.015	121.086	120.870	120.783	420.264	421.481
$\{n3,l2\}$	121.100	121.139	120.971	120.854	420.468	421.641
	121.084	121.121	120.952	120.842	420.258	421.478
$\{n3,l2,4s\}$	121.101	121.139	120.971	120.856	420.475	421.642
	121.085	121.121	120.952	120.843	420.265	421.479
$\{n3,l2,4s,4p\}$	121.102	121.140	120.972	120.857	420.471	421.641
	121.087	121.122	120.953	120.845	420.261	421.477
$\{n4,l3\}$	121.103	121.139	120.973	120.858	420.470	421.640
	121.087	121.122	120.953	120.846	420.260	421.477
$\{n4,l3,5s\}$	121.103	121.139	120.972	120.858	420.474	421.641
	121.087	121.121	120.953	120.846	420.263	421.478
$\{n4,l3,5s,5p\}$	121.104	121.139	120.973	120.860	420.474	421.642
	121.088	121.122	120.954	120.847	420.264	421.478
$\{n4,l3,5s,5p,5d\}$	121.103	121.139	120.973	120.859	420.471	421.640
	121.087	121.122	120.954	120.847	420.261	421.477
$\{n5,l4.\}$	121.104	121.139	120.973	120.859	420.472	421.640
	121.088	121.122	120.954	120.847	420.262	421.477
$\{n5,l4,6s,6p\}$	121.104	121.139	120.973	120.859	420.472	421.640
	121.088	121.122	120.954	120.847	420.261	421.477

ing coefficients and we expect that the above active set takes into account all the important correlation configurations.

III. RESULTS AND DISCUSSION

The energy levels of the initial and final configurations under consideration can be identified without ambiguity in the *LS* coupling and *jj* coupling schemes for low and high-Z elements, respectively. However for medium Z ions, neither of these notations classify the states unambiguously. Hence our present usage of energy ordering to classify the states with *LSJ* notation cannot be taken seriously.

Our calculations show that the influence of limited mixing between the 15 correlation configurations on the single configuration DF energies of the $K\beta$ x rays is marginal and varies from 0.0003 Å to 0.0006 Å. The transition energies with contributions from Breit interaction, QED effects, and correlation are nearly the same as the energies calculated with contribution from only correlation.

To analyze the effects of limited correlation from 15 CSFs and Breit interaction on the single configuration rates, the $K\beta$ x-ray rates from states of $2s3p$ configuration are listed in Table I for a few selected elements. The first row of each element corresponds to the monoconfiguration DF rates, second row to the rates with only correlation, and the third row to the rates with correlation and Breit interaction. The correlation effect enhances the single configuration DF rates from $^3P_{0,1,2}$-$^3S_1$ transitions in general and the increase in DF rates ranges from $\sim$2.5% to 3.8% for ions with $Z \leq 23$. As Z increases, the difference between the two rates decreases and the enhancement in the rates varies from 1.8% for $Z=24$ to 0.5% for $Z=54$. The dipole rates with contributions from Breit interaction, QED effects, and correlation are nearly the same for these transitions as the rates calculated with the inclusion of only correlation. For $^1P_1$-$^1S_0$ transition, higher order corrections marginally reduce the DF rates in ions with $Z>23$ whereas correlation slightly enhances the DF rates The influence of Breit interaction on the DF rates is appreciable for spin-forbidden transitions and the relativistic corrections enhance the DF rates more than the correlation

TABLE III. RCI wavelengths of $K\beta$ x rays in Å with correlation from 505 CSFs. Also listed are the relativistic MZ wavelengths [22].

Z	$^1P_1$-$^1S_0$	$^3P_1$-$^3S_1$	$^3P_0$-$^3S_1$	$^3P_2$-$^3S_1$	$^1P_1$-$^3S_1$	$^3P_1$-$^1S_0$
14	5.3548	5.3074	5.3055	5.3062	5.3166	5.3456
	5.3509	5.3071	5.3052	5.3062		
16	4.0833	4.0515	4.0503	4.0505	4.0576	4.0773
	4.0809	4.0514	4.0502	4.0505		
17	3.6107	3.5842	3.5831	3.5833	3.5892	3.6058
	3.6087	3.5841	3.5830	3.5832		
18	3.2151	3.1929	3.1921	3.1920	3.1970	3.2110
	3.2138	3.1929	3.1921	3.1920		
20	2.5962	2.5803	2.5797	2.5794	2.5831	2.5933
	2.5955	2.5802	2.5797	2.5784		2.5926
21	2.3482	2.3378	2.3373	2.3369	2.3402	2.3492
	2.3485	2.3377	2.3373	2.3369		2.3485
22	2.1399	2.1277	2.1273	2.1269	2.1299	2.1377
	2.1392	2.1277	2.1273	2.1269		2.1372
23	1.9535	1.9446	1.9443	1.9438	1.9433	1.9521
	1.9547	1.9446	1.9443	1.9438		1.9529
24	1.7919	1.7841	1.7838	1.7832	1.7827	1.7905
	1.7930	1.7841	1.7838	1.7832		1.7914
25	1.6480	1.6425	1.6424	1.6416	1.6411	1.6493
	1.6504	1.6425	1.6422	1.6416		1.6490
26	1.5232	1.5170	1.5168	1.5161	1.5156	1.5218
	1.5240	1.5170	1.5168	1.5161		1.5228
27	1.4106	1.4052	1.4051	1.4044	1.4038	1.4096
	1.4115	1.4052	1.4050	1.4043		1.4104
28	1.3105	1.3052	1.3052	1.3044	1.3039	1.3089
	1.3109	1.3052	1.3051	1.3044		1.3100
32	0.9971	0.9951	0.9950	0.9941	0.9938	0.9984
	0.99699	0.99504	0.9950	0.99414	0.99376	0.99829
34	0.8803	0.8776	0.8789	0.8780	0.8789	0.8816
	0.88093	0.87946	0.87944	0.87853	0.87820	0.88220
36	0.7838	0.7827	0.7827	0.7817	0.7814	0.7850
	0.78375	0.78266	0.78265	0.78171	0.78143	0.78499
40	0.6327	0.6297	0.6309	0.6299	0.6309	0.6315
42	0.5717	0.5691	0.5703	0.5693	0.5703	0.5705
44	0.5201	0.5175	0.5187	0.5177	0.5187	0.5189
48	0.4345	0.4322	0.4333	0.4323	0.4334	0.4334
50	0.3992	0.3970	0.3982	0.3971	0.3982	0.3980
52	0.3679	0.3658	0.3670	0.3659	0.3670	0.3667
54	0.3400	0.3381	0.3392	0.3381	0.3392	0.3389

effect.

In the following pages, the $K\beta$ x-ray wavelengths and rates calculated with 505 correlation configurations generated from the active set with $n=1$ to 6 Layzer complex are reported and analyzed with the limited configuration interaction arising from 15 CSFs generated from the reference configurations. In Table II, sample data analyzing the effect of SD excitations on the converged MCDF and RCI energies of $J=1$ states from $2s3p$ and $J=0,1$ states from $1s2s$ configurations of He-like iron are reported. The active set in column 1 lists the orbitals included in the set. For example, $\{n3,l2\}$ means that the set consists of $\{1s_{1/2},2s_{1/2},2p_{1/2},2p_{3/2},3s_{1/2},3p_{1/2},3p_{3/2},3d_{3/2}3d_{5/2}\}$ orbitals. The first row of energies in the gradually expanding set includes only correlation while the second row represents correlation as well contributions from higher order corrections. All the energies listed in this table are negative values. It is clear from Table II that the active set with 505 CSFs is

TABLE IV. RCI electric dipole rates of $K\beta$ x rays in s^{-1} in length gauge with correlation from 505 CSFs. The relativistic MZ rates [22] are also included. The numbers in parentheses signify powers of ten.

Z	$^1P_1$-$^1S_0$	$^3P_0$-$^3S_1$	$^3P_2$-$^3S_1$	$^3P_1$-$^3S_1$	$^1P_1$-$^3S_1$	$^3P_1$-$^1S_0$
14	3.629(12)	3.322(12)	4.751(12)	3.294(12)	4.201(9)	2.951(10)
	2.82(12)	2.61(12)	4.67(12)	3.55(12)		
16	6.033(12)	6.064(12)	8.649(12)	6.115(12)	1.447(10)	9.354(10)
	4.90(12)	4.97(12)	8.44(12)	6.46(12)		
17	7.572(12)	7.992(12)	1.123(13)	8.097(12)	2.568(10)	1.547(11)
	6.26(12)	6.66(12)	1.10(13)	8.50(12)		
18	9.169(12)	9.990(12)	1.394(13)	1.061(13)	4.310(10)	2.425(11)
	7.86(12)	8.77(12)	1.4(13)	1.1(13)		
20	1.365(13)	1.685(13)	2.264(13)	1.710(13)	1.248(11)	5.317(11)
	1.18(13)	1.45(13)	2.2(13)	1.77(13)		4.67(11)
21	1.578(13)	2.024(13)	2.672(13)	2.085(13)	1.847(11)	7.684(11)
	1.41(13)	1.82(13)	2.7(13)	2.2(13)		6.68(11)
22	1.868(13)	2.554(13)	3.292(13)	2.615(13)	2.988(11)	1.023(12)
	1.66(13)	2.27(13)	3.28(13)	2.71(13)		9.29(11)
23	1.012(13)	3.126(13)	3.967(13)	3.179(13)	8.307(12)	1.430(12)
	1.94(13)	2.79(13)	3.96(13)	3.29(13)		1.27(12)
24	1.183(13)	3.782(13)	4.723(13)	3.817(13)	1.175(13)	1.906(12)
	2.23(13)	3.39(13)	4.73(13)	3.94(13)		1.69(12)
25	1.629(13)	4.518(13)	5.563(13)	4.525(13)	1.358(13)	2.470(12)
	2.54(13)	4.09(13)	5.61(13)	4.69(13)		2.22(12)
26	2.207(13)	5.388(13)	6.549(13)	5.331(13)	1.594(13)	3.242(12)
	2.87(13)	4.890(13)	6.620(13)	5.520(13)		2.890(12)
27	2.891(13)	6.339(13)	7.614(13)	6.199(13)	1.849(13)	4.066(12)
	3.21(13)	5.79(13)	7.75(13)	6.44(13)		
28	3.734(13)	7.452(13)	8.855(13)	7.182(13)	2.171(13)	5.278(12)
	3.58(13)	6.82(13)	9.03(13)	7.46(13)		4.70(12)
32	8.515(13)	1.327(14)	1.523(14)	1.197(14)	3.986(13)	1.265(13)
	8.53(13)	1.23(14)	1.58(14)	1.25(14)	3.87(13)	1.13(13)
34	1.182(14)	1.722(14)	1.948(14)	1.49(14)	5.310(13)	1.872(13)
	1.200(14)	1.600(14)		2.050(14)	1.570(14)	5.250(13)
36	1.577(14)	2.199(14)	2.457(14)	1.840(14)	6.965(13)	2.694(13)
		2.06(14)	2.61(14)	1.93(14)	7.00(13)	
40	2.577(14)	3.447(14)	3.766(14)	2.683(14)	1.141(14)	5.158(13)
42	3.193(14)	4.244(14)	4.585(14)	3.196(14)	1.426(14)	6.889(13)
44	3.897(14)	5.175(14)	5.528(14)	3.780(14)	1.759(14)	9.012(13)
48	5.598(14)	7.499(14)	7.812(14)	5.194(14)	2.582(14)	1.461(14)
50	6.612(14)	8.923(14)	9.161(14)	6.042(14)	3.079(14)	1.818(14)
52	7.749(14)	1.054(15)	1.064(15)	6.999(14)	3.641(14)	2.233(14)
54	9.016(14)	1.238(15)	1.225(15)	8.073(14)	4.270(14)	2.710(14)

sufficient enough to incorporate the important correlation configurations.

Our calculations show that for He-like ions with $Z<18$, the correlation effect lowers the energy of the $^1P_1$ state substantially as a consequence of which the $^1P_1$ state becomes more negative than the $^3P_1$ state thereby inverting the structure of the $^3P_1$ and $^1P_1$ states with limited correlation. For example, the energy values of $^3P_1$ and $^1P_1$ states of Si^{2+} with 15 correlation configurations are −34.284 880 a.u. and −34.204 353 a.u., respectively. With additional correlation contributions resulting from 505 CSFs, the converged energies of $^3P_1$ and $^1P_1$ states become −34.362 812 a.u. and −34.501 225 a.u., respectively. As the active space expands, the major contribution to the mixing coefficients of the $2s3p_{1/2}$ (or $2s3p_{3/2}$) $J=1$ state is from $2p_{1/2}3s$ $J=1$ state instead of the expected $2s3p_{3/2}$ (or $2s3p_{1/2}$) $J=1$ state. The $2s3p_{1/2}$ (or $2s3p_{3/2}$) $J=1$ admixture to the $2s3p_{3/2}$ (or $2s3p_{1/2}$) $J=1$ becomes the next appreciable contribution to

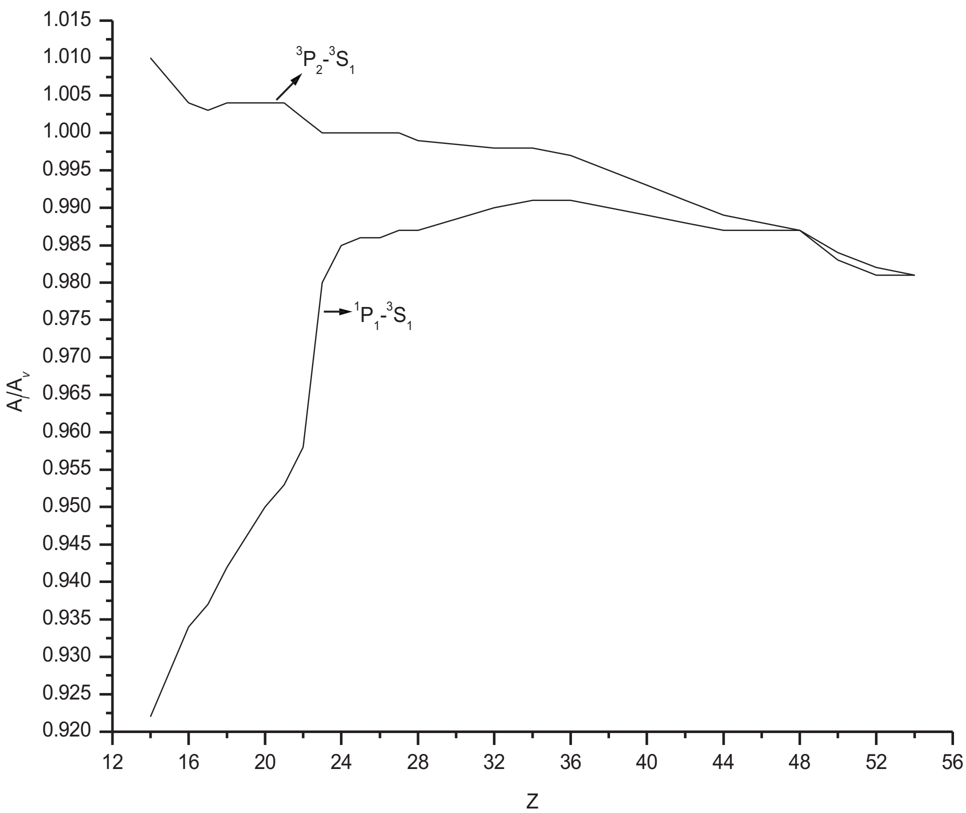

FIG. 1. Length to velocity ratios of RCI rates ($\frac{A_l}{A_v}$) as a function of Z.

mixing coefficients. The mixing coefficients of the $J=1$ states from $2s3p_{3/2}$ and $2p_{1/2}3s$ configurations are nearly the same for $Z<18$. However, the strength of correlation of the $2p_{1/2}3s$ $J=1$ state with the $2s3p_{1/2}$ $J=1$ state is less in comparison to that of $2s3p_{3/2}$ with $2p_{1/2}3s$ $J=1$ state and this results in the inversion of the $^3P_1$ and $^1P_1$ states. Though the $2p_{1/2}3s$ admixture to $2s3p_{1/2}$ $J=1$ state decreases with increasing Z and the energy of the $^3P_1$ state becomes more negative than the $^1P_1$ state thereby retaining the LS coupling energy ordering, it is seen that for all ions considered in this work, the $2p_{1/2}3s$ admixture to $2s3p_{3/2}$ state is stronger than that from $2s3p_{1/2}$ state. The contributions from higher order corrections to the energies of the multiplet states are negligible for light elements and in the case of Si^{12+}, the energy values of $^3P_1$ and $^1P_1$ states due to correlation and higher order corrections are −34.361 049 a.u. and −34.508 942 a.u., respectively. With increasing Z, the contribution from relativistic corrections also increases.

Our present investigation shows an anomalous behavior in the mixing coefficients of $2s3p_{3/2}$ $J=1$ state for ions with $Z=18$ to 22. For example, the significant correlation contributions to the $2s3p_{1/2}$ $J=1$ state of $Z=20$ are 0.7561, 0.4278, 0.3672, 0.2686, and 0.1286 from the $J=1$ states of $2s3p_{1/2}$, $2p_{1/2}3s$, $2s3p_{3/2}$, $2p_{3/2}4s$, and $2p_{3/2}4d_{3/2}$ configurations, respectively whereas the dominant contributions to the $2s3p_{3/2}$ $J=1$ state are from $2p_{1/2}3s$, $2s3p_{3/2}$, $2s3p_{1/2}$, $2p_{3/2}3s$, and $2p_{3/2}3d_{3/2}$ with respective 0.6091, 0.5202, 0.4442, 0.3514, and 0.1917 coefficients. For ions with $Z>22$, while the contributing correlation configurations retain the same structure for $2s3p_{1/2}$ $J=1$ state, the first few mixing states to the $2s3p_{3/2}$ $J=1$ state in the decreasing order of contributions are $2s3p_{3/2}$, $2p_{1/2}3s$, $2p_{3/2}3s$, $2p_{3/2}3d_{5/2}$, $2p_{3/2}3d_{3/2}$, etc. It is also observed that for ions with $Z>22$, the $2s3p_{3/2}$ $J=1$ state does not have any appreciable contribution from the expected $2s3p_{1/2}$ $J=1$ state.

The RCI wavelengths of the $K\beta$ x rays from states of $2s3p$ configuration of ions in the range $Z=14$ to 54 are listed in Table III. Also included are the wavelengths for various transitions reported by Goryayev and Vainshtein [22] using relativistic MZ expansion method. To the best of our knowledge, no experimental results on the x rays from $2s3p$ configuration of He-like ions are reported so far. The present wavelengths are in excellent agreement with the MZ values of Goryayev and Vainshtein [22] for $^3P_{0,1,2}$-$^3S_1$ transitions. The present energies are in fair agreement with the MZ values for the $^1P_1$-$^1S_0$ transition in low Z elements. With increasing Z, the difference between the two results decreases and a good agreement is found between the two wavelengths. The $^3P_1$-$^1S_0$ spin-forbidden transition energies differ from the MZ values by ~0.009 Å for $Z<30$. For higher Z, the energies from the $^3P_1$-$^1S_0$ and $^1P_1$-$^3S_0$ transitions are in very good agreement with the MZ values.

The length gauge RCI rates for the allowed and spin-forbidden dipole transitions are listed in Table IV for various Z. Also listed in this table are the E1 rates from MZ calculations of Goryayev and Vainshtein [22]. It is seen from Table IV that the $^1P_1$-$^3S_1$ transition starts out as a weak transition and is much smaller than the $^3P_1$-$^1S_0$ transition for low Z elements. However, at $Z=23$, a sharp increase in the $^1P_1$-$^3S_1$ transition rate is noticed and reaches an order of magnitude larger than the $^3P_1$-$^1S_0$ rate. It is also seen that at $Z=24$, the $^1P_1$-$^3S_1$ transition rate is nearly the same as the allowed $^1P_1$-$^1S_0$ rate and with increasing Z, it becomes a relatively strong transition. The RCI rates are slightly larger

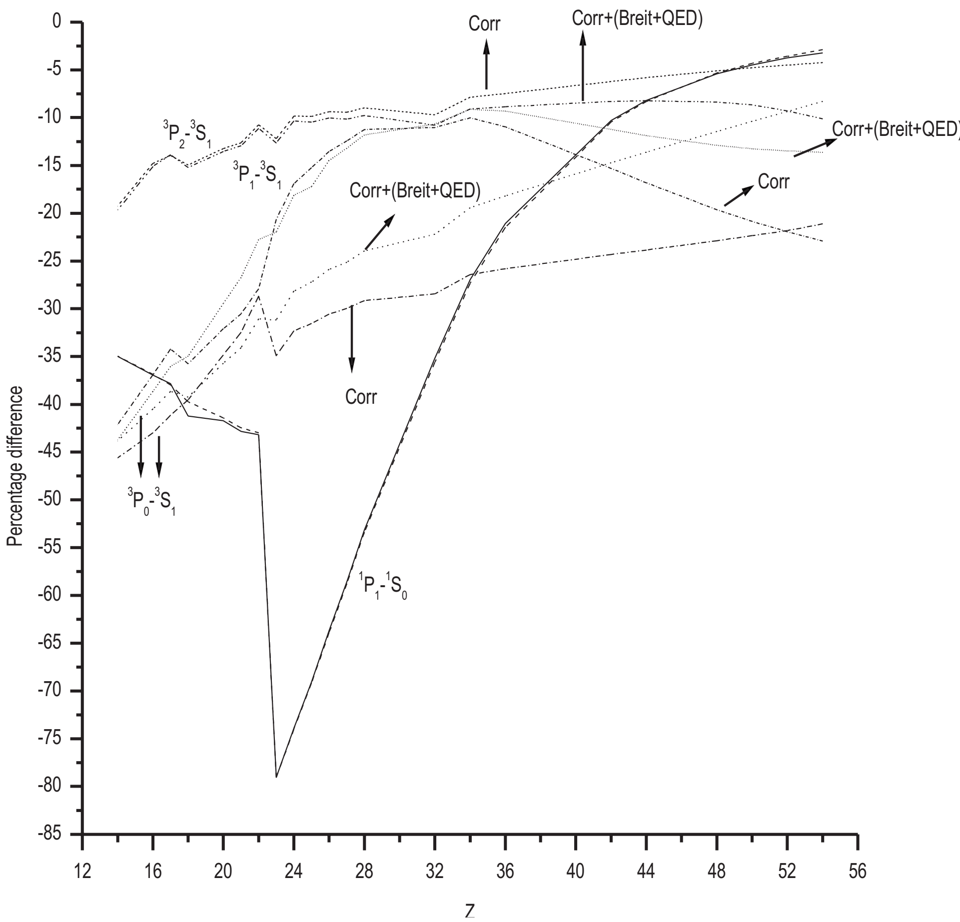

FIG. 2. Effects of correlation, Breit interaction, and QED corrections on the allowed E1 rates of $K\beta$ lines from states of $2s3p$ configuration in He-like ions as functions of atomic number. The curves denoted as Corr.+(Breit+QED) indicate the percentage differences between the rates calculated with large and limited correlation configurations along with contributions from Breit interaction and QED effects. The curves specified as Corr. represent the percentage differences between the rates calculated with large and limited correlation configurations without the contributions from Breit interaction and QED effects.

than the MZ rates for $^3P_0$-$^3S_1$ transition in all ions whereas they are marginally smaller than MZ values for $^3P_1$-$^3S_1$ transition. The present $^3P_2$-$^3S_1$ transition rates are in very good agreement with the MZ rates with a maximum difference of ~3.5%. The $^1P_1$-$^1S_0$ rates reported in this work are slightly larger than the MZ rates for ions with $Z \leq 23$ and are smaller for other high-Z elements. The spin-forbidden transition rates are also in good agreement with the MZ rates. The differences between our present RCI rates and the relativistic MZ rates [22] are partly due to the differences in the wave functions and partly due to the approach used in this work in the evaluation of correlation effects.

Our calculations show that the ratios of RCI dipole allowed rates in length and velocity forms (A_l/A_v) for various transitions to $^1S_0$ and $^3S_1$ states are nearly unity in the mid-Z region. The length rates are marginally larger than the velocity rates for low Z elements and slightly smaller for high-Z elements. The A_l/A_v values of the spin-forbidden rates range from 0.996 to 1.01 for $^3P_1$-$^1S_0$ transition whereas for the $^1P_1$-$^3S_1$ transition, they vary from 0.925 to 0.991. The A_l/A_v values for $^3P_2$-$^3S_1$ and $^1P_1$-$^3S_1$ transitions are plotted in Fig. 1 for various Z. The general trend of the curves suggests the level of accuracy of the wave functions used in the present work.

Though the dipole rates of the allowed and spin-forbidden transitions listed in Table IV vary smoothly with Z, the effects of correlation and relativistic corrections on the E1 rates exhibit a nonsmooth behavior. To analyze in detail the characteristics of the various radiative transitions considered in this work, the percentage differences between the length gauge dipole rates of x rays calculated with multiconfiguration sets with 505 CSFs and limited configuration set with 15 CSFs with respect to the latter rates are explored in Figs. 2 and 3 for allowed and forbidden transitions, respectively. These two CSF sets include Breit interaction and QED effects. To analyze the effect of only correlation on the dipole rates, similar length gauge percentage differences between the dipole rates calculated with large (505 CSFs) and limited (15 CSFs) correlation configurations without Breit interaction and QED effects are also plotted in these figures. Our calculations show that correlation and higher order corrections reduce the limited configuration rates of dipole allowed as well as $^3P_1$-$^1S_0$ transitions (Fig. 3). However, these effects enhance spin-forbidden rates of $^1P_1$-$^3S_1$ transition in ions with $Z \geq 23$ and reduce the rates of low Z ions by as much as 94%. While the reduction in the rate is consistent, the enhancement which is abrupt and steep at $Z=23$ decreases rapidly between $Z=25$ to 34 and the variation is nearly a constant beyond this region. The allowed $^1P_1$-$^1S_0$ transition also shows a sharp discontinuity at $Z=23$. The reduction in the $^1P_1$-$^1S_0$ rate ranges from 35% to 45% for ions with $Z=14$ to 22. However, the reduction is well pronounced (~78%) at $Z=23$. As Z increases, the difference between the $^1P_1$-$^1S_0$ transition rates with large and limited configuration interaction decreases rapidly to ~13% at $Z=40$ and at $Z=54$ the difference is a mere 3% indicating the fact that the strength

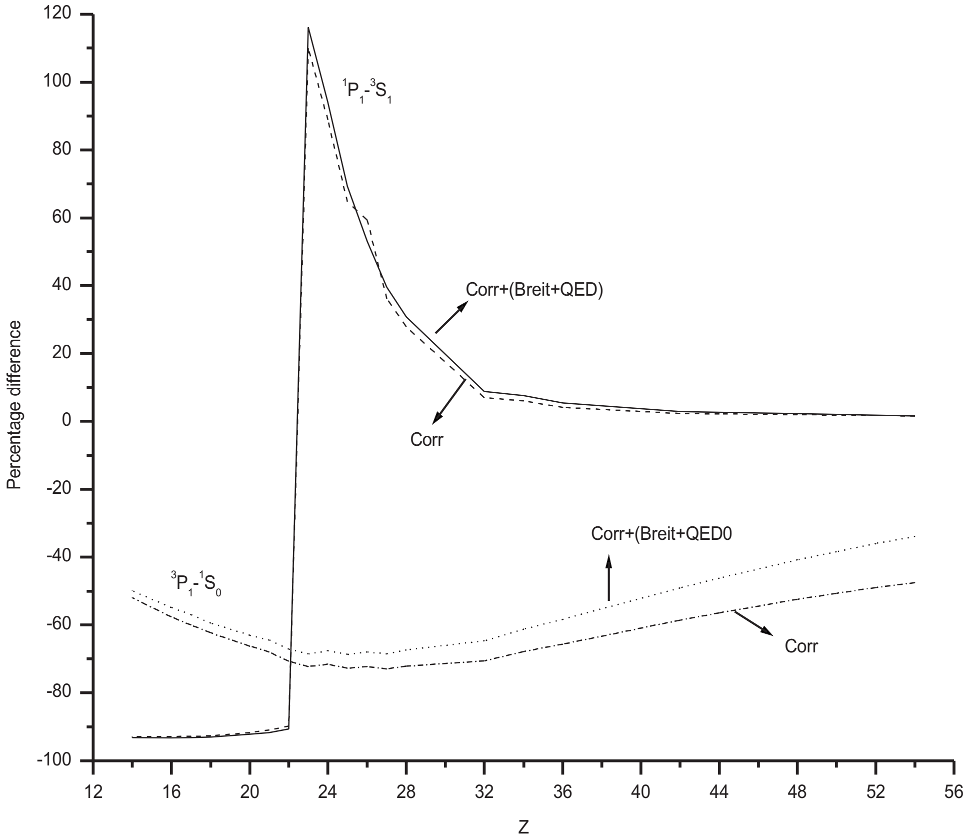

FIG. 3. Percentage differences for spin-forbidden transitions. The legends are the same as in Fig. 2.

of correlation on the dipole rates is only marginal for high-Z elements. The influence of correlation on the other allowed E1 rates is significant for low Z elements and decreases in general with increasing Z. It is also seen that the strength of correlation on the $^3P_0$-$^3S_1$ transition is in general nearly double those of the other two transitions from $^3S_1$ state. In the case of $^3P_1$-$^1S_0$ transition, the reduction in the rate is 50% at $Z=14$, reaches a maximum of $\sim$75% in the range with $Z=23$ to 26, and thereon the reduction varies gradually. The contribution from the most important relativistic effects to the $^1P_1$-$^1S_0$ rate is negligible while its effect is noticeable on the other transition rates. The Breit interaction reduces the $^3P_2$-$^3S_1$ rate further by $\sim$2% for all ions considered in this work and the same reduction is observed in the case of $^3P_1$-$^3S_1$ rates with low Z. However, the Breit interaction enhances the MCDF rates of $^3P_1$-$^3S_1$ transition by 2% for ions in the range $Z=30$ to 40. As Z increases, the difference between contributions to the x-ray rates from correlation and Breit interaction increases from 3% at $Z=42$ to 8% at $Z=56$. The effect of Breit interaction on the $^1P_1$-$^3S_1$ rate is significant and it in general enhances the MCDF rates by $\sim$10%. The nonsmooth variations in the percentage differences show that the correlation and relativistic contributions depend on the type of transition and also on the atomic number. The dip or shoot up in the percentage differences observed at $Z=23$ in Figs. 2 and 3 might probably be due to the irregular contributions to the mixing coefficients of the $2s3p_{3/2}$ $J=1$ state.

IV. CONCLUSION

The wavelengths and rates of x rays from $2s3p$ configurations of He-like ions with $Z=14$ to 54 reported in this work reveal that correlation effects alter significantly the single configuration rates and contribution from limited configuration mixing is not sufficient to predict the expected rates. It is noticed that the strength of electron-electron correlation on the dipole rates varies with the type of transition considered and is also Z dependent. The influence of Breit interaction on the transition rates is marginal for a few transitions and is in general appreciable for allowed transitions from $^3S_1$ and spin-forbidden transition from $^1S_0$ states of high-Z elements.

ACKNOWLEDGMENT

This work was supported by the project financed by the Department of Science and Technology, Government of India, New Delhi, India

[1] K. J. H. Phillips, C. D. Pikes, J. Lang, T. Watanbe, and M. Takahashi, Astrophys. J. **435**, 888 (1994).
[2] V. Desclaux, P. Beiersdofer, S. M. Kahn, and V. L. Jacobs, Astrophys. J. **482**, 1076 (1997).
[3] J. F. Seely, Phys. Rev. Lett. **42**, 1606 (1979).
[4] E. Kallne, J. Kallne, E. S. Marmar, and J. E. Rice, Phys. Scr. **31**, 551 (1985).
[5] V. A. Boiko, A. Ya Faenov, S. A. Pikuz, I. Yu Skobelev, A. V. Vinogradov, and E. A. Yokov, J. Phys. B **10**, 3387 (1977).
[6] P. Beiersdorfer, M. Bitter, S. von Goeler, and K. W. Hill, Phys. Rev. A **40**, 150 (1989).
[7] M. Bitter, H. Hsuan, V. Decaux, B. Grek, K. W. Hill, R. Hulse, L. A. Kruegel, D. Johnson, S. von Goeler, and M. Zarnstorff, Phys. Rev. A **44**, 1796 (1991).
[8] P. Beiersdorfer, M. Bitter, D. Hey, and K. J. Reed, Phys. Rev. A **66**, 032504 (2002).
[9] A. J. Smith, M. Bitter, H. Hsuan, K. W. Hill, S. von Goeler, J. Timberlake, P. Beiersdorfer, and A. Osterheld, Phys. Rev. A **47**, 3073 (1993).
[10] J. E. Rice, M. A. Graf, J. L. Terry, E. S. Marmar, K. Geising, and F. Bombarda, J. Phys. B **28**, 893 (1995).
[11] J. P. Mosnier, R. Barchewitz, M. Cukier, R. Dei-cas, C. Senemaud, and J. Bruneau, J. Phys. B **19**, 2531 (1986).
[12] A. Langenberg, R. L. Watson, and J. R. White, J. Phys. B **13**, 4193 (1980).
[13] M. R. Tarbutt, R. Barnsley, N. J. Peacock, and J. D. Silven, J. Phys. B **34**, 3979 (2001).
[14] M. H. Chen, B. Crasemann, and H. Mark, Phys. Rev. A **26**, 1441 (1982).
[15] K. R. Karim and L. Logan, Phys. Scr. **58**, 574 (1998).
[16] H. Lin, C. S. Hsue, and K. T. Chung, Phys. Rev. A **65**, 032706 (2002).
[17] H. Y. Yang and K. T. Chung, Phys. Rev. A **51**, 3621 (1994).
[18] Igor Yu. Skobelev *et al.*, Phys. Rev. E **55**, 3773 (1997).
[19] K. R. Karim and C. P. Bhalla, Phys. Rev. A **34**, 4743 (1986).
[20] C. P. Bhalla and K. R. Karim, Nucl. Instrum. Methods Phys. Res. **57**, 2005 (1986).
[21] C. P. Bhalla, K. R. Karim, and T. Reeves, Phys. Scr. **34**, 747 (1986).
[22] F. F. Goryayev and L. A. Vainshtein, e-print arXiv:physics/0603164.
[23] L. Natarjan and Anuradha Natarjan, Phys. Rev. A **75**, 062502 (2007).
[24] C. Froesce Fischer, T. Brage, and P. Jonnson, *Computational Atomic Structure* (IOP, Bristol, 1997).
[25] P. Jonsson, X. He, and C. F. Fischer, Technical Report DOE/ER/US, 1998 (unpublished).
[26] K. G. Dyall, I. P. Grant, C. T. Johnson, F. A. Parpia, and E. P. Plummer, Comput. Phys. Commun. **55**, 425 (1989).
[27] I. P. Grant, B. J. McKenzie, P. H. Norrington, D. F. Mayers, and N. C. Pyper, Comput. Phys. Commun. **21**, 207 (1980).
[28] Y.-K. Kim, D. H. Baik, P. Indelicato, and J. P. Desclaux, Phys. Rev. A **44**, 148 (1991).
[29] Anuradha Natarajan and L. Natarajan, J. Phys. B **37**, 4789 (2004).
[30] Anuradha Natarajan and L. Natarajan, J. Quant. Spectrosc. Radiat. Transf. **109**, 2281 (2008).